Proceedings of the Canadian Society for Mechanical Engineering International Congress
32nd Annual Conference of the Computational Fluid Dynamics Society of Canada
Canadian Society of Rheology Symposium
CSME-CFDSC-CSR 2025
May 25–28, 2025, Montréal, Québec, Canada

Thermogravimetric Analysis of Refuse-Derived Fuel and Its Sorted Fractions Under Torrefaction Conditions

Oluwaseunnla P. Adelusi[12*], Micael Boulet[2], Stéphane Moreau[1]
[1]Department of Mechanical Engineering, University of Sherbrooke, Sherbrooke, QC, Canada
[2]Enerkem Inc, Sherbrooke, QC Canada
*Oluwaseunnla.P.Adelusi@USherbrooke.ca

Abstract—Highlighting the rejects of the rejects, this study focuses on refuse-derived fuels (RDF) generated from non-recyclable municipal solid waste. Unlike wood or coal gasification, RDF in its natural state is a poor fuel source, containing different types of materials, such as paper and plastic, which exhibit distinct chemical properties, thermal properties, and energy content. The efficiency of RDF gasification is limited by its heterogeneity. To enhance the yield and efficiency of the gasification process, torrefaction is being considered as a pre-treatment process. Due to the difficulty of predicting the impact of thermochemical processes on RDF, a monitoring system is required to better understand and control the macro-composition of individual fractions. In this study, RDF fractions are studied independently towards modelling a relation between the percentage composition of each RDF individual fraction and the effects of torrefaction. These include papers, plastics, cardboard, other organics, and fines (<1 cm), which made up more than 90% of the RDF as received from waste sorting centres. Through thermogravimetric analysis, the effects of torrefaction on mass loss have been obtained for all fractions at 200°C, 250°C, 300°C, and 350°C. Using the main RDF fractions, a recombined RDF was produced and torrefied in this study. Instead of a synergistic effect, an additive effect was observed when comparing the mass loss obtained in the recombined RDF to the expected theoretical mass loss computed based on the composition of each fraction and its individual mass losses. From 200°C to 300°C, the experimental and theoretical values closely align, with absolute differences of only 0.74%, 0.04%, and 0.28% at 200°C, 250°C, and 300°C, respectively.

Keywords- Torrefaction; Municipal Solid Waste (MSW); Refuse-Derived Fuels (RDF); Thermogravimetric Analysis (TGA)

I. INTRODUCTION

Recent years have witnessed advancements in technologies for producing bioenergy from various biomass sources, including municipal solid waste (MSW). Considering global waste management challenges, energy generation from waste provides a solution to two prominent climate change issues [1]. This study focuses on energy generation from waste, specifically, the unrecyclable portion of MSW, refuse-derived fuel. The valorization of refuse-derived fuels (RDF) poses a significant challenge owing to its high heterogeneity and constantly varying chemical and physical composition. Other challenges with energy generation from RDF include the low calorific value, low mass density, poor grindability, poor flow behaviour, and presence of contaminants [2,3]. Different thermochemical conversion processes can be applied to RDF and biomasses; the most prominent are combustion, gasification, carbonization, pyrolysis, and torrefaction [4–6].

Gasification produces synthesis gas (syngas) from carbonaceous materials derived from fossil fuels or non-fossil organic sources such as biomasses. This thermochemical process has been applied to transform RDF into syngas and processed into biofuels and other renewable energy products [7,8]. To improve the efficiency of RDF gasification, researchers have recommended torrefaction as a pre-treatment process [2,9–11].

Figure 1. Schematic Principle of Torrefaction

Torrefaction, a low-energy-demanding thermochemical process, occurs between 200°C and 350°C and has been applied to different types of biomasses with the goal of upgrading its properties such as energy density, grindability, and other characteristics. The key parameters for evaluating torrefaction include mass and higher heating value (HHV). In Figure 1, M represents the Mass Yield, and E_r denotes the Energy Density Ratio, which is the ratio of the HHV of the product to that of the raw RDF [12,13].

In studies from Kerdsuwan et al. [14], Abdulyekeen et al. [15], and Mamvura et al. [16], torrefaction resulted in an energy yield of between 101.31% and 107.78% for RDF, organics in MSW, and other biomasses. Similarly, the effect of torrefaction on gasification has been recorded in multiple studies to result in increased cold gas efficiency and decreased tar content of the syngas [2,9,17,18]. For high-efficiency gasification, feedstock flexibility and feeding systems are strong factors in the process design based on the influence of optimizing gasification yields. Hence, torrefaction as a feedstock pre-treatment process requires deeper understanding to be integrated into the gasification process.

The heterogeneity of RDF remains a challenge in designing systems to manage, predict, and control the composition of RDF. To completely understand RDF thermal, chemical, and flow behaviour, it is vital to throw light on the fractions, also called macro-compositions. This study presents the first data characterizing the effects of torrefaction on complete independent RDF fractions, and the theoretical formulations represent a step forward in estimating torrefaction severity.

II. RDF Fractions

The macro-composition of RDF involves the individual fractions that can be sorted manually, such as paper, plastic, and wood, according to the ASTM-D5231–92–2016. In this study, a series of material processing steps were conducted to obtain a representative sample of RDF from barrels generated at the City of Edmonton Integrated Processing and Transfer Facility (IPTF), Canada. The materials processing and preparation are described in a prior study of Rashwan et al. [19] and entail the quartering technique, according to ASTM C702, and grinding (to <1 mm), according to ASTM E829-16.

A. *Fractions and Percentage Compositions*

Two batches of RDF were manually sorted, and the fractions were evaluated to obtain an estimation of the amounts of each fraction present in each representative sample from each batch. In both batches received in 2021 and 2023, the primary fractions were cardboard, papers, plastics, other organics, and fines (<1 cm). These made up approximately 94% to 98% of each batch, with the remaining portion consisting of wood, metals, glass, and other organics as shown in Figure 2. Fractions and their composition of RDF affect the overall thermal property, which makes it crucial to understand the fractions and their effect on torrefaction severity.

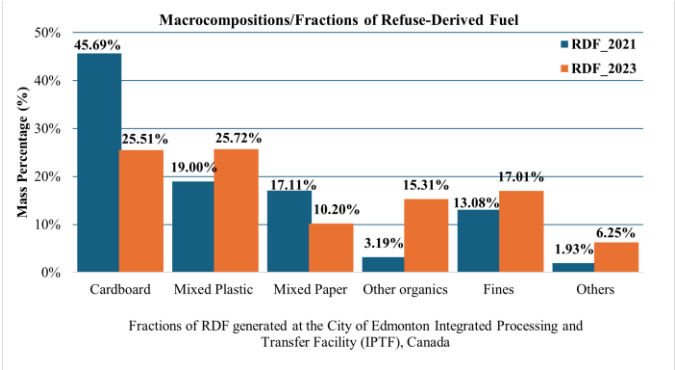

Figure 2. Fractions of RDF generated at the City of Edmonton Integrated Processing and Transfer Facility (IPTF), Canada

Unlike previous research [20,21] that simulated RDF contents with pure materials or incomplete representations of RDF fractions, this project involves the torrefaction of all of the RDF fractions separately. From the study of Bar-Ziv and coworkers [22,23], blends of paper, plastics, and fibres revealed a synergistic effect during torrefaction. This study considers a more representative RDF composition in the test sample, allowing a more wholesome investigation of the synergistic effect during torrefaction, measured through thermal properties.

B. *Recombined RDF*

In order to have an accurate comparison of the fractions to the RDF, the pulverized fractions were recombined to create a more controlled sample, RDF_r. Therefore, the proportions were recalculated, and RDF_r comprises cardboard, papers, plastics, other organics, and fines in quantities corresponding to the normalized composition.

III. Torrefaction by Thermogravimetric Analyzer

Thermogravimetric analysis (TGA) has been used in several studies for analysing MSW and RDF to study thermochemical processes like pyrolysis [21] and torrefaction of MSW and biomasses respectively [24,25]. This study applies the TGA as it allows precise control of temperature, sequencing for isotherm (residence time), inert environment, and varying heating rates as required for torrefaction experiments. The torrefaction experiment involves three main steps sketched in Figure 3:

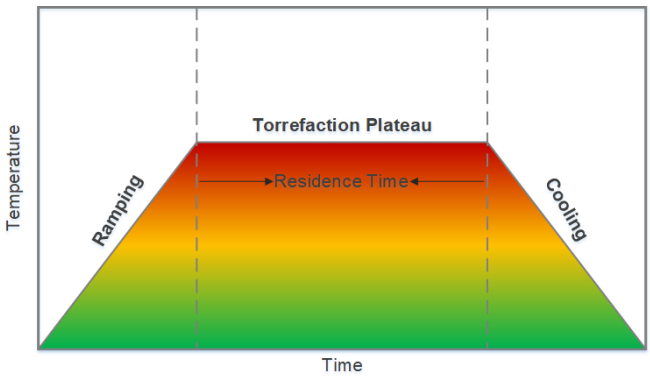

Figure 3. Typical Heating Profile in Torrefaction Experiments

1) Ramping: In this stage, the RDF is heated at a slow rate of 5–20°C/min to reach the intended torrefaction temperature.

2) Torrefaction Plateau: For 30 minutes, which represents the residence time, the RDF sample remains at the torrefaction temperaure to allow for decomposition of the sample.

3) Cooling: The TGA allows for rapid cooling or slower cooling as desired. However, this study does not focus on the cooling stage due to the minimal sample size. Furthermore, no major chemical or mass changes are observed after the torrefaction plateau.

IV. Experimental Procedure

All six RDF fractions and RDF_r were torrefied at four temperatures: 200°C, 250°C, 300°C, and 350°C. The SDT 650 DSC/TGA Simultaneous Thermal Analyzer was used for this study. The device allows for the selection of a predefined sequence for the three stages of torrefaction. In these experiments, the sample mass ranged between 1 to 5 mg while the heating rate was set to 10°C/min, and nitrogen gas was used to create the inert environment.

V. Results and Discussions

The thermogravimetric analysis was conducted and repeated following the same procedure for each experimental case. The mass loss curves presented in Figures 4 through 7 show the retained mass (or mass yield) on the left y-axis with the mass loss at the end, beside each curve. Based on the TGA torrefaction sequence, it takes 17, 23, 27, and 32 minutes to reach the torrefaction temperature of 200°C, 250°C, 300°C, and 350°C respectively, resulting in a total experimental duration of 47 to 62 minutes.

A. Torrefaction at 200°C

In Figure 4, the mass loss, for all fractions, increased progressively with temperature, with significant thermal decomposition occurring beyond 250°C. At 200°C, thermal degradation was minimal, as the mass loss across all materials remained below 7.5%. Mass loss at this stage is majorly due to the loss of moisture which is present more in organic fractions like cardboards and papers than in plastics. This explains the 1.4% mass loss in plastics and is also confirmed in the mass loss rates and derivative curves, which have just one tiny peak at 105°C. Similar peaks were obtained in the study from Rashwan et al. [19].

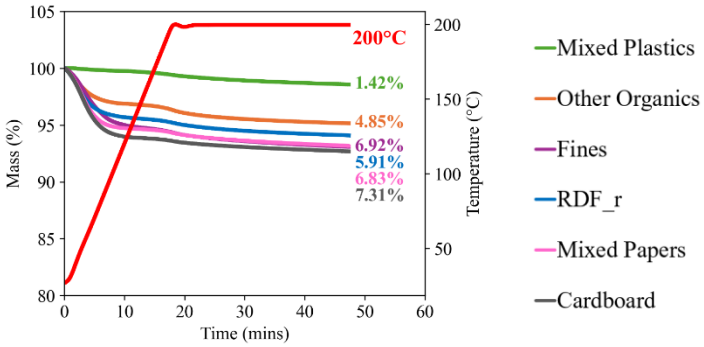

Figure 4. TGA Mass Loss Profile of RDF: Torrefaction at 200°C

Cardboard showed the highest mass loss at all temperatures, suggesting that cellulosic materials are slightly more susceptible to low-temperature degradation compared to plastics.

B. Torrefaction at 250°

From 250°C, thermal degradation begins to occur as seen in the second dip in the mass loss curves in Figure 5. This dip starts around 200°C, and the mass for all fractions reduces progressively until the end the residence time. The mass loss rate is lowest with plastics in all temperature cases, while cardboard and papers have higher mass loss rates after 200°C. The studies from Rashwan et al. [19] and Xu et al. [22] also noted similarly increasing mass loss rates. The organic-based fractions, such as cardboard (14.82%) and mixed papers (14.63%), show a more pronounced decomposition indicative of the onset of hemicellulose degradation [4,19,21]. The recombined RDF, RDF_r, has a mass loss of 11.14%, which falls in between mixed plastics and cardboard or mixed papers, confirming the effect of both fractions in the RDF.

Fines in RDF are the contents below 1 cm separated using a standard sieve. Unlike the RDF_r, at 250°C torrefaction, the fines fraction has a mass loss of 13.58%, close to the values for cardboards and mixed papers. This implies that the fines contain more of the organic fractions, although all fractions of RDF are usually in fines. The difference between mass loss in RDF_r and fines also confirms the composition of fines to be more organic materials, where decomposition can be observed from temperatures around 200°C and above.

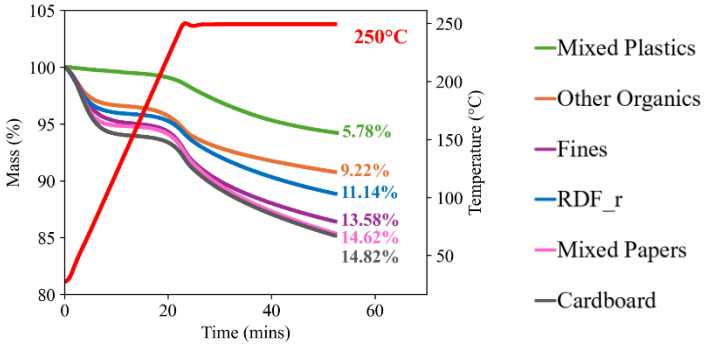

Figure 5. TGA Mass Loss Profile of RDF: Torrefaction at 250°C

Other organics contain textiles, rubber, leather, clothes, and other unlisted combustibles as defined by ASTM-D5231–92–2016. With a mass loss of 9.22%, other organics exhibit a mass loss lower than other organic-based fractions like cardboard and mixed papers as well as RDF and fines. This is indicative of plastic components being included in the other organic fraction during the sorting and reveals insights on the reliability of manual RDF sorting methods. Although the sorting follows standard methods, the manual procedure is subject to human error. For example, certain rubber, leather, or textile waste materials are often fused to—or made in mix with—plastic materials.

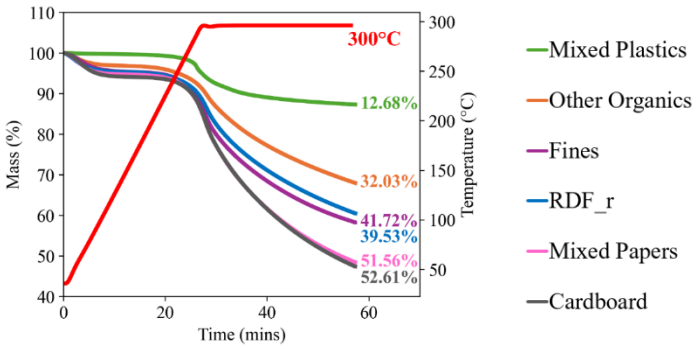

Figure 6. TGA Mass Loss Profile of RDF: Torrefaction at 300°C

C. *Torrefaction from 300°C to 350°C*

From 300°C, there is a sharp rise in mass loss as seen in Figures 6 and 7, particularly in the organic-rich fractions. Cardboard and mixed papers experienced a higher decomposition rate than other fractions with a mass loss of over 50%. For both fractions, the mass loss at 300°C was over three times the values at 250°C and seven times the values at 200°C. This relates to the breakdown of the lignocellulosic components, cellulose and hemicellulose, as seen with the rapid peak in the mass loss rates. Also confirmed in different studies, these components decompose more rapidly as temperature rises towards ≈360°C, which is the peak temperature corresponding to the maximum decomposition rate for both papers and cardboard [19,20]. At 350°C the mass loss further increases to 82.17% and 75.65% for cardboard and mixed papers, respectively. Hence, the majority of mass loss occurs within the 300°C–350°C threshold as seen in the trends in Figure 8.

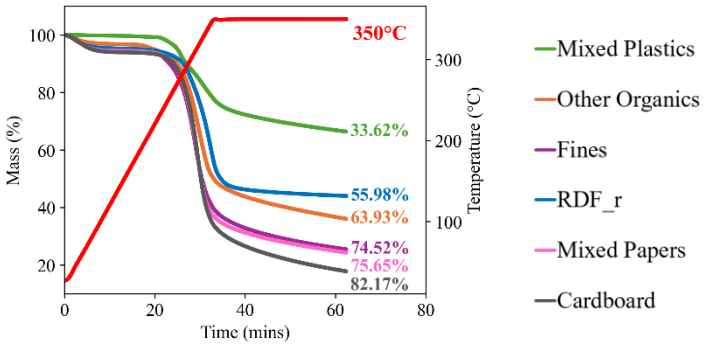

Figure 7. TGA Mass Loss Profile of RDF: Torrefaction at 350°C

Mixed plastics also experienced more mass loss within the 300°C–350°C threshold, although the maximum mass loss (33.62%) falls far from the other fractions. Figure 8 shows that 83% of the 33.62% mass loss recorded occurred during this threshold, alluding to the absence of any decomposition at lower temperatures. The mass loss falls within the first (200°C–335°C) and second (335°C–400°C) decomposition stages for mixed plastics, which was recorded in the study from Rashwan et al. [19]. Despite the lack of focus on torrefaction or residence time, the present results can be related to this study in considering the mass loss rates. The mass loss corresponds to the initial degradation of polyethylene, polyvinyl chloride, polypropylene, and polystyrene in the mixed plastics. Miandad et al. [26] also confirm this in their study on plastics in waste.

At 300°C, the mass loss for other organics increased rapidly from the 250°C value (9.22%) to reach 33.62%. This value doubled by 350°C, rising to 63.93%. As initially indicated above, the organic fractions seem to be contaminated by some components of plastics, suggesting the difference in the trends of other organics from papers and cardboard.

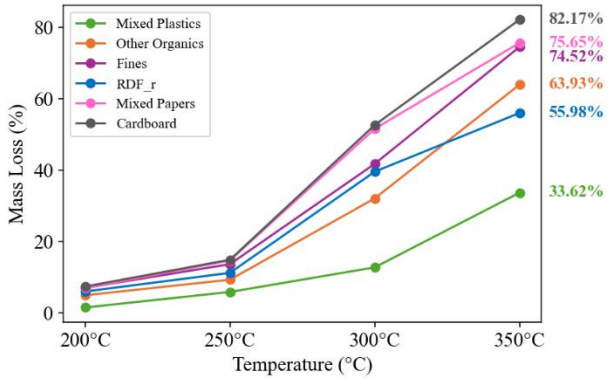

Figure 8. Mass Loss Trends Across Torrefaction Temperatures

It is important to also note the divergence of values for papers and cardboard at 350°C in Figure 7. In their differential thermal analysis (DTA) of cardboard and paper, Rashwan et al. found that the profiles of both materials almost perfectly overlapped, with a peak decomposition temperature of about 360°C. However, the peak is deeper, with cardboard having a maximum decomposition rate of about −25%/min and paper, about −20%/min. Hence, as the curves diverge from around 340°C until around 380°C, there is a slightly elevated mass loss rate in cardboards. This explains the divergence in the curves for cardboard and papers in Figure 7. In terms of composition, cardboard contains higher cellulose and lignin content, which decomposes later, while hemicellulose would have been decomposed from 220–315°C [27].

Similar to other fractions, RDF_r and Fines have a rapid mass loss from 250°C to 300°C, increasing by a difference of about 28% to a value four times the prior temperature. This shows that more mass loss occurs at the higher temperatures. Figure 8 shows that RDF and fines have similar mass loss trends from 200°C to 300°C with a deviation at 350°C. This indicates that the fines have a similar composition to the RDF. However, RDF shows an increase in mass loss from 39.5% to 55.98%, and Fines, 41.72% to 74.52%, indicative of a reduced mass loss rate in the RDF as the temperature increases from 300°C to 350°C. This variation can be attributed to the presence of more cellulosic organic materials present in the fines and decomposing later on, within the 315–400°C temperature range [27]. Furthermore, organic materials like plants and wood can also be found within the fine fraction as the dried materials break and fall within the <1 cm particle size.

D. *Effects of Inter-fraction Interaction on Mass Loss*

The theoretical mass loss for RDF_r was computed using linear mixing rules. Hence, it is a weighted summation of individual fraction mass losses based on their relative composition in the recombined RDF (RDF_r). Figure 9 shows that the experimental values aligned with the expected theoretical mass loss until 350°C. Here, the mass loss obtained

experimentally was lower than the expected value, indicative of an antagonistic effect in contrast to the study from Xu et al. [22], which recorded insignificant interaction effects. The results suggest that inter-fraction interactions are insignificant in terms of mass loss at 200°C–300°C torrefaction temperatures.

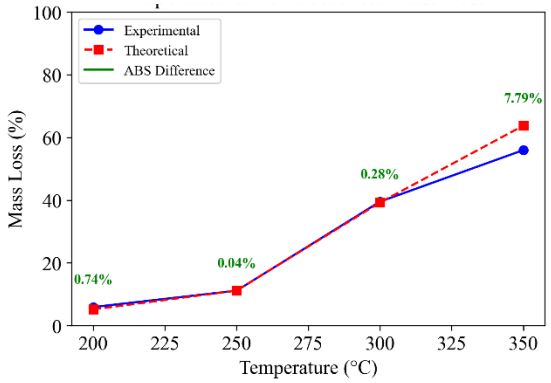

Figure 9. Experimental vs Theoretical (Calculated) Mass Loss

VI. Conclusion

This study provides critical insights into the behaviour of refuse-derived fuel (RDF) and its individual fractions during torrefaction, towards addressing the challenges posed by RDF heterogeneity. The thermogravimetric analysis (TGA) revealed distinct thermal decomposition patterns for the different RDF fractions. The results indicate that at lower torrefaction temperatures (200°C–250°C), mass loss is primarily due to moisture evaporation and the initial degradation of hemicellulose. At higher temperatures (300°C–350°C), significant mass loss occurs, particularly in cellulosic fractions such as cardboard and paper, while plastics experience a delayed but notable degradation. While cardboards and papers show overlapping trendlines from 200°C to 300°C, the mass loss differs slightly at 350°C, with cardboard being higher due to its composition and the higher decomposition rate from 340°C.

The study shows the lowest mass yield at all temperatures to correspond to cardboard and paper, with the plastic fractions having the most mass retained after torrefaction. Furthermore, for all fractions, the mass loss is most significant after 300°C, accounting for a higher percentage of the total mass loss.

The recombined RDF (RDF_r) exhibits an additive rather than a synergistic effect in mass loss, aligning closely with the theoretical mass loss values at 200°C–300°C. However, at 350°C, a divergence is observed, suggesting potential antagonistic interactions among RDF fractions. This deviation highlights the complexity of RDF composition and underscores the necessity for further investigations into inter-fraction interactions during torrefaction.

The findings of this study contribute to a deeper understanding of RDF fractions and their behaviour during torrefaction. It explores the relationship between RDF properties and the composition levels of each fraction, providing insights for predicting torrefaction severity. Future work will consider other crucial parameters for torrefaction severity, such as the higher heating value and energy density. By addressing these aspects, the inter-fraction interaction can be investigated in terms of energy and chemical transformation, which would be beneficial for developing prediction models for RDF torrefaction.

Acknowledgment

The authors would like to acknowledge the support of the University of Sherbrooke and the industrial partner, Enerkem Inc., where the manual sorting and sample preparation was performed.

References

[1] Bioenergy - IEA n.d. https://www.iea.org/energy-system/renewables/bioenergy (accessed November 9, 2023).

[2] Recari J, Berrueco C, Puy N, Alier S, Bartrolí J, Farriol X. Torrefaction of a solid recovered fuel (SRF) to improve the fuel properties for gasification processes. Appl Energy 2017;203:177–88. https://doi.org/10.1016/j.apenergy.2017.06.014.

[3] Sarquah K, Narra S, Beck G, Bassey U, Antwi E, Hartmann M, et al. Characterization of Municipal Solid Waste and Assessment of Its Potential for Refuse-Derived Fuel (RDF) Valorization. Energies (Basel) 2023;16. https://doi.org/10.3390/en16010200.

[4] Basu, Prabir. Biomass Gasification, Pyrolysis and Torrefaction: Practical Design and Theory. 2013.

[5] Amer M, Elwardany A, Amer M, Elwardany A. Biomass Carbonization. Renewable Energy - Resources, Challenges and Applications 2020. https://doi.org/10.5772/INTECHOPEN.90480.

[6] Osman AI, Mehta N, Elgarahy AM, Al-Hinai A, Al-Muhtaseb AH, Rooney DW. Conversion of biomass to biofuels and life cycle assessment: a review. Environ Chem Lett 2021;19. https://doi.org/10.1007/s10311-021-01273-0.

[7] Marie-Rose SC, Chornet E, Lynch D, Lavoie JM. From biomass-rich residues into fuels and green chemicals via gasification and catalytic synthesis. WIT Transactions on Ecology and the Environment 2011;143:123–32. https://doi.org/10.2495/ESUS110111.

[8] Haydary J. Gasification of Refuse-Derived Fuel (RDF). GeoScience Engineering 2016;62:37–44. https://doi.org/10.1515/GSE-2016-0007.

[9] Laohalidanond K, Kerdsuwan S, Burra KRG, Li J, Gupta AK. Syngas generation from landfills derived torrefied refuse fuel using a downdraft gasifier. Journal of Energy Resources Technology, Transactions of the ASME 2021;143. https://doi.org/10.1115/1.4048523.

[10] Nobre C, Gonçalves M, Longo A, Vilarinho C, Mendes B. Gasification of pellets produced from blends of biomass wastes and refuse derived fuel char. ECOS 2018 - Proceedings of the 31st International Conference on Efficiency, Cost, Optimization, Simulation and Environmental Impact of Energy Systems, University of Minho; 2018.

[11] Rashwan SS, Adelusi O, Boulet M, Moreau S. Turning trash into treasure: A comprehensive review on torrefaction of refuse-derived fuel from an industrial perspective. Energy Convers Manag 2025;326:119516. https://doi.org/10.1016/J.ENCONMAN.2025.119516.

[12] Rashwan SS, Boulet M, Moreau S. Maximizing Waste-to-Energy Potential: Optimizing Batch Torrefaction Reactor of Refuse-Derived Fuel for Efficient Gasification. Journal of Energy Resources Technology, Part A: Sustainable and Renewable Energy 2025;1:1–24. https://doi.org/10.1115/1.4066104.

[13] EVALUATION OF GUIDE PARAMETERS FOR BATCH TORREFACTION EXPERIMENTS OF REFUSE-DERIVED FUEL - CSME/CFDCanada2023 n.d. https://event.fourwaves.com/csme2023/abstracts/7cb74a6a-7e6c-47b4-bb80-efd3aa23e973 (accessed September 15, 2023).

[14] Kerdsuwan S, Laohalidanond K, Gupta Ashwani K. Upgrading Refuse-Derived Fuel Properties from Reclaimed Landfill Using Torrefaction. Journal of Energy Resources Technology, Transactions of the ASME 2021;143. https://doi.org/10.1115/1.4047979.

[15] Abdulyekeen KA, Daud WMAW, Patah MFA, Abnisa F. Torrefaction of organic municipal solid waste to high calorific value solid fuel using batch reactor with helical screw induced rotation. Bioresour Technol 2022;363. https://doi.org/10.1016/j.biortech.2022.127974.

[16] Mamvura TA, Pahla G, Muzenda E. Torrefaction of waste biomass for application in energy production in South Africa. S Afr J Chem Eng 2018;25:1–12. https://doi.org/10.1016/J.SAJCE.2017.11.003.

[17] Fan Y, Tippayawong N, Wei G, Huang Z, Zhao K, Jiang L, et al. Minimizing tar formation whilst enhancing syngas production by integrating biomass torrefaction pretreatment with chemical looping gasification. Appl Energy 2020;260. https://doi.org/10.1016/j.apenergy.2019.114315.

[18] Chen Q, Zhou JS, Liu BJ, Mei QF, Luo ZY. Influence of torrefaction pretreatment on biomass gasification technology. Chinese Science Bulletin 2011;56. https://doi.org/10.1007/s11434-010-4292-z.

[19] Rashwan SS, Boulet M, Moreau S. Navigating the depths of refuse-derived fuel in Canada: From heterogeneity to insightful analysis. Energy Sources, Part A: Recovery, Utilization, and Environmental Effects 2024;46:14387–403. https://doi.org/10.1080/15567036.2024.2412817.

[20] Rago YP, Collard FX, Görgens JF, Surroop D, Mohee R. Torrefaction of biomass and plastic from municipal solid waste streams and their blends: Evaluation of interactive effects. Fuel 2020;277. https://doi.org/10.1016/j.fuel.2020.118089.

[21] Ansah E, Wang L, Shahbazi A. Thermogravimetric and calorimetric characteristics during co-pyrolysis of municipal solid waste components. Waste Management 2016;56. https://doi.org/10.1016/j.wasman.2016.06.015.

[22] Xu Z, Kolapkar SS, Zinchik S, Bar-Ziv E, Ewurum L, McDonald AG, et al. Bypassing Energy Barriers in Fiber-Polymer Torrefaction. Front Energy Res 2021;9. https://doi.org/10.3389/fenrg.2021.643371.

[23] Zinchik S, Xu Z, Kolapkar SS, Bar-Ziv E, McDonald AG. Properties of pellets of torrefied U.S. waste blends. Waste Management 2020;104. https://doi.org/10.1016/j.wasman.2020.01.009.

[24] Grycova B, Pryszcz A, Krzack S, Klinger M, Lestinsky P. Torrefaction of biomass pellets using the thermogravimetric analyser. Biomass Convers Biorefin 2021;11. https://doi.org/10.1007/s13399-020-00621-4.

[25] Jamro IA, Khoso S, Shah SAR, Ali S, Ali F, Hassane HU. Investigation of Thermal Decomposition and Gases Release from Pre-Drying Municipal Solid Waste (PMSW) Via Pyrolysis Technology. Architecture, Civil Engineering, Environment 2022;15. https://doi.org/10.2478/acee-2022-0043.

[26] Miandad R, Rehan M, Barakat MA, Aburiazaiza AS, Khan H, Ismail IMI, et al. Catalytic pyrolysis of plastic waste: Moving toward pyrolysis based biorefineries. Front Energy Res 2019;7. https://doi.org/10.3389/fenrg.2019.00027.

[27] Yang H, Yan R, Chen H, Lee DH, Zheng C. Characteristics of hemicellulose, cellulose and lignin pyrolysis. Fuel 2007;86. https://doi.org/10.1016/j.fuel.2006.12.013.